ICAS 2016
30th Congress of the International Council of the Aeronautical Sciences
DCC, Daejeon, Korea ; September 25-30, 2016

DESIGN AND TEST OF THE HIGH AERODYNAMIC PERFORMANCE LOW-NOISE FAN FOR 5.5- BY 4-M ACOUSTIC WIND TUNNEL

QuXiaoli, Yu Yongsheng, Liao Daxiong, Yang Gaoqiang, Chen Qin, Tang Gengsheng

Facility Design and Instrumentation Institute, China Aerodynamics Research and Development Center, Mianyang Sichuan 621000, P. R. China
qxl@cardc.cn

Keywords: *High performance, Low noise, Fan, Acoustic, Wind tunnel*

Abstract

The arbitrary vortex method and some noise control methods are employed to design a high aerodynamic performance low noise axial fan in a 5.5- by 4-m acoustic wind tunnel. In the design process, better distribution of the axial velocity at the outlet of the fan stator is obtained by regulating the distribution of swirl velocity, and the noise generated by the fan is reduced by more reasonably matched rotor-stator blade number, stator backward-swept angle and rotor-stator spacing. The aerodynamic test results show that the wind speed required in the solid wall test section is satisfied, and when the fan rotational speed is 330rpm, the fan reaches the highest aerodynamic efficiency (95.7%) and the fan section also has the highest aerodynamic efficiency (90%). Moreover, the acoustic test results show that the Overall Sound Pressure Level (OASPL) at the fan inlet is 101 dB(A), and the OASPL at the fan outlet is 105 dB(A) when the wind speed in the open jet test section reaches 80m/s. The combination of the arbitrary vortex method with noise control methods is proved to be a good design approach for the axial fan of large acoustic wind tunnel.

NOMENCLATURE

Symbols:

r	Radius (mm)
c	Chord (mm)
x	Dimensionless radius
N	Rotational speed (rpm)
u	Axial velocity (m/s)
ε_s	Dimensionless swirl speed
U	Mean velocity in fan plane (m/s)
Cl	Lift coefficient
λ_s	Advance ratio
σ	Solidity
β	Blade setting angle (deg)
η_f	Fan-section efficiency
η_b	Fan efficiency
G	Mass flow rate (kg/s)
g	Volume flow rate (m^3/s)
F	Fan power (w)
T_0	Total temperature at fan plane (K)
P_T	Total pressure (Pa)

Subscripts:

0	Upstream of fan section
1	Just upstream of fan rotor
2	Just downstream of fan rotor
3	Just downstream of fan stator
4	Downstream of fan section
s	Between rotor and stator
U	Reference velocity in fan plane

1 Introduction

Acoustic wind tunnel with very low background noise level is an important and very useful facility for aerodynamic sound measurement in developing quieter and more comfortable airplanes and vehicles. The major noise source in such a wind tunnel is the fan. The fan blade passing frequency and fan blade/stator interaction contribute to the tonal background noise in the test section, and the broadband fan noise is also an important source of broadband background noise[1]. To reduce the contribution of fan noise to the background noise in the test section, reduction of the fan noise and attenuation of the propagation of fan noise in the wind tunnel circuit are considered. If a fan with lower noise is available, more acoustic liner and other acoustic treatments will not be needed, and the cost of an acoustic wind tunnel can be lower. Meanwhile, a fan with high aerodynamic performance can reduce the power required for the operation of wind tunnel and improve the flow qualities in the test section. Hence the design technology of low noise fan with high aerodynamic performance is a key technology in the design of aero-acoustic wind tunnel.

In the aerodynamic design of axial fan, the free vortex design method and the arbitrary vortex method are two widely used methods, and both require the assumption of two-dimensional flow. The free vortex method is widely used in the design of axial fan which satisfactorily meets the design requirements of low speed wind tunnel, mine ventilation system, and cooling system, and the details of this method have been described by Collar [2], Pope [3] and Wallis [4]. This method also assumes that the flow velocity has no radial component, and the theoretical axial velocity and the total pressure rise of the fan are both constant along the fan radius. In contrast, the arbitrary vortex method does not require radial equilibrium and a real velocity distribution can be applied in the fan design procedure [5]. Moreover, fan design with higher aerodynamic performance can be achieved with this method. For example, Van Ditshuizen [6] used this method to design the pilot fan of NLR LST, whose efficiency reached 92%.

Many methods have been proposed to reduce fan noise. The most famous design rule regarding fan geometry is the Tyler-Sofrin rotor-stator selection criterion [7], which is useful to get a cut-off blade passing frequency to reduce interaction noise. Large axial distance between the fan rotor blades and stator blades is also widely adopted as an effective method in passive control of fan noise [8-9], although the extended rotor-stator spacing may slightly influence the aerodynamic performance of the fan and increase the overall weight of the fan system. Stator sweep and/or lean have been proved to reduce the severity of the interaction between the rotor and stator and suppress the tonal noise [10-12]. Taking the advantages of fan noise reduction methods mentioned above, Moreau[13] successfully reduced the broadband fan noise by 2dB compared with the original noise in the NWB wind tunnel by equipping a swept stator with low blade count.

This paper presents the design methods and validation tests for the axial fan in the 5.5- by 4-m acoustic wind tunnel in China Aerodynamics Research and Development Center (CARDC). This low speed aero-acoustic wind tunnel with closed circuit has a solid wall test section and an open jet test section, hence requiring a fan system with high quality aerodynamic and acoustic performances. To achieve such high aerodynamic performance, the arbitrary vortex method is employed to optimize the geometry of fan rotor and stator blades, and various noise reduction methods are used to reduce the fan noise.

2 Fan Design

2.1 Design Requirements

The acoustic wind tunnel (Figure 1) has two test sections, one with solid wall and the other with open jet. The dimensions of the test section are 5.5m x 4m (width x height), and the maximum speeds of the solid wall and open jet test

sections are 130 m/s and 100 m/s, respectively. The required OASPL of the background noise is 75-80 dB(A) at the wind speed of 80m/s [14] (calculated based on the 1/3rd octave spectrum in the frequency range of 200 Hz to 20 kHz of the sound pressure signal recorded at the location 5m downstream of the nozzle exit and 7.95 m away from the central axis of the test section in the horizontal medial plane).

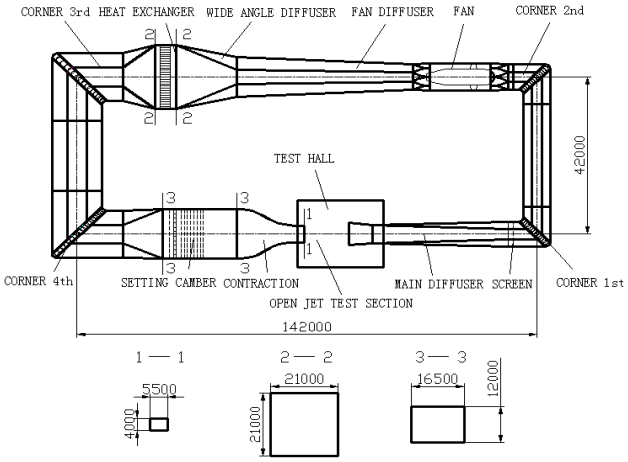

Fig. 1 The outline of 5.5×4m acoustic wind tunnel

For an acoustic wind tunnel, the contribution of fan noise is required to be as small as possible to the background noise level in the test section.

According to the plan made by the lead aerodynamicist of this acoustic wind tunnel, the specific fan design requirements are listed below in Table 1.

Table 1 Technical requirement specification for the fan

Test Section	Wind Speed	Total Pressure Rise	Volume Rate	Fan Noise	Fan Efficiency
Solid Wall	130m/s	3100Pa	2920 m^3/s	--	≥90%
Open Jet	100m/s	3040Pa	2200 m^3/s	--	--
Open Jet	80m/s	1950Pa	1760 m^3/s	≤110dBA	≥88%

2.2 Aerodynamic Design

The aerodynamic design aims to achieve higher fan efficiency mainly by optimizing the configurations of the rotor blades and tail cone, and other components of the fan are designed by conventional ways. After the aerodynamic design is completed, a 1/10 scaled prototype fan is developed and installed in the pilot wind tunnel of 5.5- by 4-m acoustic wind tunnel, and experiments are carried out to verify the fan design method and if the tail cone shape is optimum.

2.2.1 Fan Blade

The fan blades are designed using the arbitrary vortex method. Different from the free vortex design method, this method does not require radial equilibrium, and the swirl coefficient is not inversely proportional to the radius. Normally, the swirl coefficient has a linear distribution along the radius:

$$\varepsilon_s = ax + b \tag{1}$$

Where x is the dimensionless radius, and both a and b are constants.

Using arbitrary vortex method, the fan system can transform the oncoming skewed velocity distribution into a more uniform distribution at the rotor and stator exit by optimizing the swirl velocity component with radius. Thus the flow leaving the stator has a sufficiently uniform distribution of velocity before entering the post-fan diffuser, and the intermittent type of premature separation is avoided. Moreover, adjusting the load distribution on the blade leads to larger output work at the tip of the blade, so the fan can achieve higher efficiency at lower rotational speed.

The design point is selected corresponding to the solid wall test section with the wind speed 130m/s. The velocity upstream of the fan blades is measured on the pilot fan:

$$U_1 = (-0.47x + 1.384)U \tag{2}$$

Once the swirl velocity and the axial velocity at the fan inlet are known, the axial velocity at the fan rotor outlet and the axial velocity at the stator outlet can be obtained from the following two equations.

$$U_2 = \sqrt{\left(\frac{U_1}{U}\right)^2 + \left(\frac{2\varepsilon_s}{\lambda_s} - (\varepsilon_s)^2\right) - \left(\frac{2\varepsilon_s}{\lambda_s} - (\varepsilon_s)^2\right)_{xU} - 2\int_{xU}^{x} (\varepsilon_s)^2 dx/x} \tag{3}$$

$$U_3 = \sqrt{\left(\frac{U_2}{U}\right)^2 + (\varepsilon_s)^2 - ((\varepsilon_s)^2)_{xU} + 2\int_{xU}^{x}(\varepsilon_s)^2 dx/x} \qquad (4)$$

After the axial velocities at the fan rotor outlet and at the stator outlet (U_2 and U_3 , respectively) have been derived, the chord lengths and setting angles of the rotor and stator blades can be determined according to the detailed design procedure introduced in reference [15].

Figure 2 shows the designed profiles of axial velocity at different fan locations. By adjusting the blade loading, more uniform velocity distributions can be obtained at the rotor outlet and stator outlet. Consequently a significant redistribution of axial energy occurs in the fan plane and the momentum of the flow near the fan tip is significantly improved.

Figure 3 shows that the predicted lift coefficient increases along the radius in both the solid wall and open jet test sections. The maximum lift coefficient reaches 0.98, which is far below the blade stall lift coefficient of 1.3 (since the "Gö 797" airfoil is employed as the profile of rotor blade). Meanwhile, enough margin of fan pressure rise is available in case of increased pressure loss in the wind tunnel.

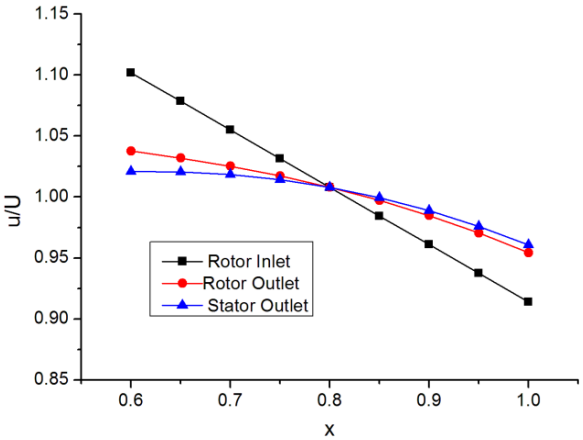

Fig. 2 Axial velocity versus x at different location

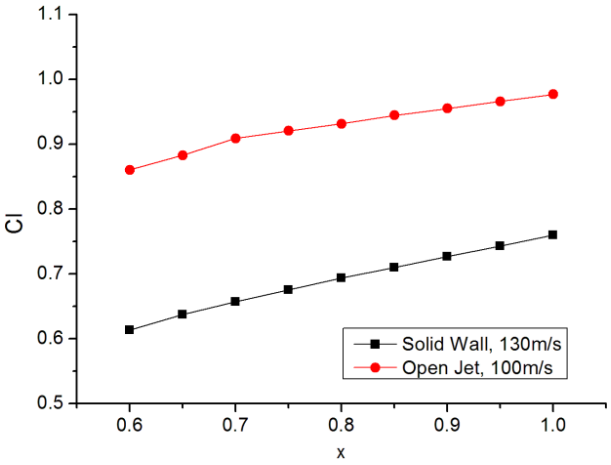

Fig.3 Lift coefficients versus x with different operating point

2.2.2 Tail Cone

A tail cone is required that is attached to the fan hub and extends rearward to the exit of the fan outlet section. The static pressure recovery in the annular diffuser downstream of the stator constitutes an important component of the overall fan pressure rise, and the flow qualities at the exit of the annular diffuser affect the flow characteristics in the downstream section (i.e. the fan diffuser downstream of the fan in the wind tunnel).

The conventional shape of tail cone is based on streamlined body of revolution, which has a conical surface. In order to obtain better pressure recovery and prevent flow separation, the equivalent diffuser angle is recommended to be 8-10 degree [16], which demands a certain length of the tail cone. However, the proposed fan has extended rotor-stator distance for noise reduction purpose, so the length of tail cone has to be cut off for a given length of fan section. Consequently, the tail cone's conical end is truncated to meet the required diffuser angle in shorter length, and pilot experiments are conducted to investigate the influences of various tail cone shapes on the fan performance.

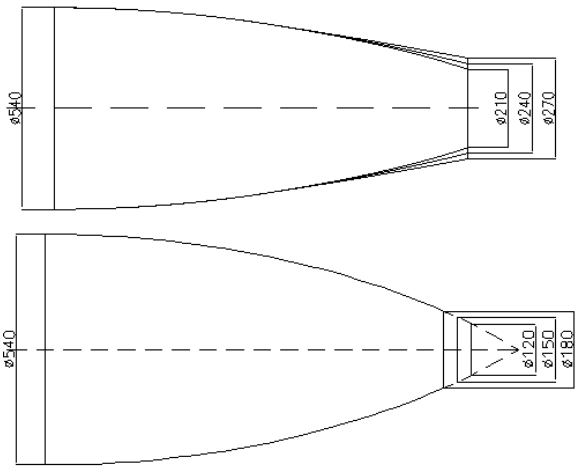

Fig.4 The modifications of tail cone

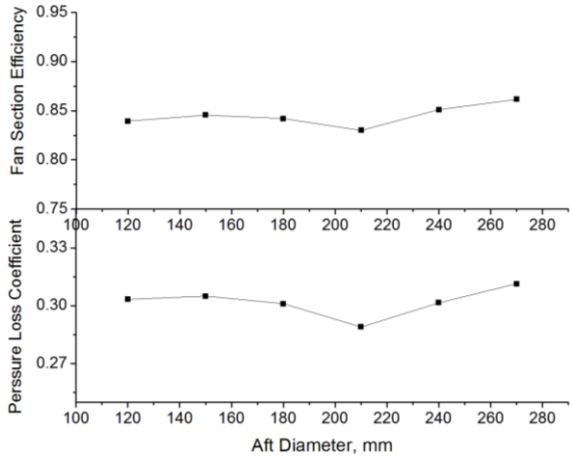

Fig. 5 The wind tunnel pressure loss coefficient and fan-section efficiency for different tail cone

Six tail cone modifications are tested in the pilot experiment, as shown in Figure 4. The truncated surface at the end of tail cone is circular, and the tested aft diameters are 120, 150, 180, 210, 240 and 270 mm. The overall wind tunnel pressure loss and the efficiency of the fan section are tested for each tail cone modification, and the results are shown in Figure 5. The fan-section efficiency changes with the increase of aft diameter, and the highest efficiency is obtained when the aft diameter is 270mm. The overall pressure loss in the wind tunnel has similar pattern of variation with the aft diameter, and the lowest pressure loss coefficient (0.289) is obtained when the aft diameter is 210mm.

The fan power is determined by the fan-section efficiency and wind tunnel pressure loss. The above results suggest that the tail cone shape not only affect the fan efficiency, but also alter the circuit pressure loss mostly by changing the internal flow in the fan diffuser. For minimizing the operational power of the 5.5- by 4-m acoustic wind tunnel, the tail cone with 210mm aft diameter is finally selected (which corresponds to the lowest circuit pressure loss coefficient), because the proposed fan efficiency can be further improved by optimizing the rotor/stator design but the configuration of the downstream fan diffuser has been fixed before the fan design starts.

2.3 Acoustics Design

In the stage of aerodynamic design, the aerodynamic performance of the fan is optimized by improving the fan efficiency and preventing flow separation at the fan tip and hub. In the stage of acoustic design, fan noise source control and fan noise level reduction are considered to develop a low noise fan based on the aerodynamic design. Because the fan is the largest noise source in the wind tunnel circuit, most efforts of noise reduction in the test section are directed at attenuating the noise generated by the fan. Other noise sources in the wind tunnel will only become important once the fan noise has been reduced to very low levels.

The control of fan noise sources is implemented in three steps. First, the numbers of rotor-stator blades are selected to eliminate the rotor-stator tonal noise by cutting-off the first blade passing mode. According to this criterion, the proposed fan should have ten rotor blades and seventeen stator blades. Second, the rotor-stator spacing is optimized to weaken the impinging wakes, and the selected axial distance between the trailing edge of the rotor blade and the leading edge of stator blade is 1.5 times the chord length of rotor blade. Third, blade sweeping introduces a spatial shift of the noise sources, which induces acoustic interferences, and substantial noise reduction can be achieved, especially for the interaction tones. Accordingly, 25-degree backward sweeping is employed on the stator blades. Meanwhile, 15-degree

backward swept tail cone supporting vanes and 15-degree forward swept nose cone supporting vanes are applied.

Acoustic treatment is used to absorb the noise radiated by various fan noise sources. All the flow surfaces within the fan inlet transition, the outlet transition and tail cone sections are acoustically treated, except for that along the nosecone. All the acoustic treatment has 600-mm thick sound absorptive material covered with perforated galvanized steel sheet on the airflow side. In all perforated sheets, holes with nominal diameters of 5 mm are located on staggered centers (45° or 60°) to form the porosity of 35%, and the thickness of the perforated sheets is 1.6 mm. The sound absorptive material is centrifugal glass wool with density of 32kg/m^3.

2.4 Design Result

The designed fan (Figure 6, Figure 7) has 9-m diameter and 0.6 hub-tip ratio, and at the selected maximum fan speed of 360 rpm, the fan power is 12.5 MW. The length of the whole fan section is 30 m, including a 6.75-m long fan inlet transition section downstream of corner 2 (Figure 1) and an 8.75-m long fan outlet transition section. A half ellipsoid with ellipticity of 2 is employed as the nosecone, and the aft diameter of the tail cone end is 2.1m, based on the result of pilot experiment. NACA0009 and NACA0012 airfoils are employed as the profiles of nose cone supporting vane and tail cone supporting vane, respectively.

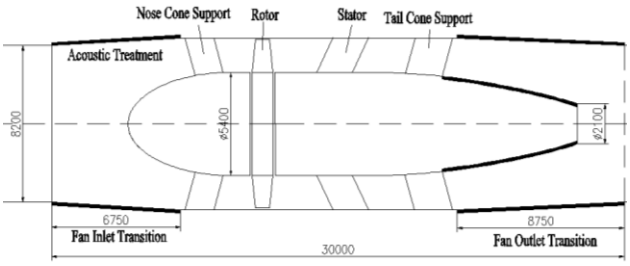

Fig. 6 Sketch designed fan of the 5.5×4m acoustic wind tunnel

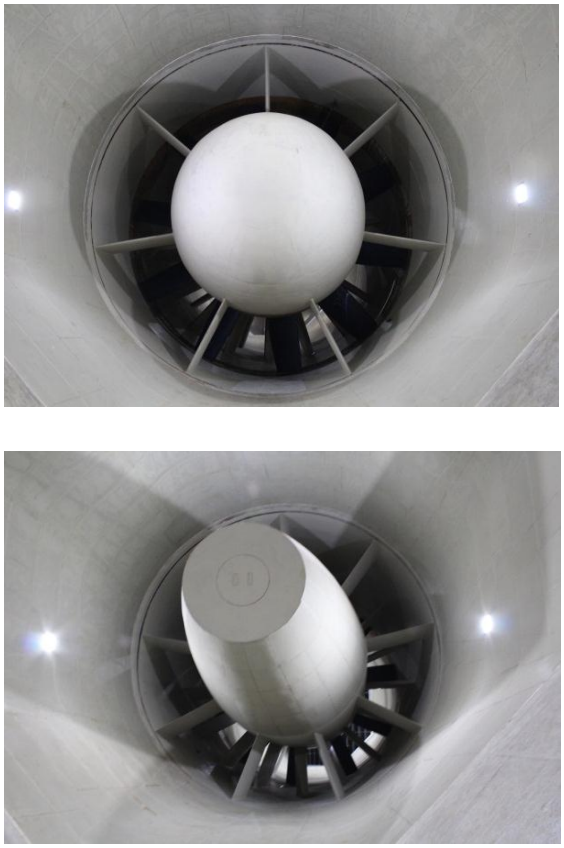

Fig.7 Photos of the fan during testing phase

The fan rotor has ten blades with “Gö797” profile over the whole blade span, and the stator has seventeen blades with NACA 4415 profile and constant chord length along the span. The distance between the rotor blades and stator blades is 1900mm, which is 1.5 time of the chord length of rotor blade. To prevent flow separation at the fan hub, the interface of the blade root and rotor hub has spherical shape so the blade-hub gap is minimized; the blade tip-casing clearance is selected to be less than 9mm, for minimizing the aerodynamic loss at the blade tip. The geometrical characteristics of the rotor and stator blades are summarized in Table 2.

Table 2 Blade cascade parameters for rotor and stator

	r(mm)	c(mm)	σ	β(deg)
Rotor Blade				
Hub	2700	1260	0.743	38.68
Mid-span	3600	1060	0.469	28.89
Tip	4500	860	0.304	22.19
Stator Blade				
Hub	2700	1850	1.85	81.5
Mid-span	3600	1850	1.39	81.5
Tip	4500	1850	1.11	81.5

3 Fan Test Description

The aerodynamic and acoustic performances of the designed fan are tested by CARDC during the wind tunnel commissioning test.

Fan-section efficiency and fan efficiency are two important indexes for evaluating the fan aerodynamic performance. Different equations are used to calculate the two indexes more exactly:

The fan-section efficiency is defined by Eq. (5)

$$\eta_f = \frac{g\cdot(P_{0T}-P_{4T})}{F} \tag{5}$$

The fan efficiency is defined by Eq. (6), which follows as

$$\eta_b = \frac{G\cdot 1004.5\cdot T_0\cdot\left[(P_{3T}/P_{1T})^{2/7}-1\right]}{F} \tag{6}$$

Two total pressure rakes are installed at the inlet and outlet of the fan section and each rake consists of forty-one steel tubes with 2-mm internal diameters and located at 200-mm intervals. Two other total pressure rakes are installed upstream of the rotor blade and downstream of the stator blade and each rake consists of seventeen steel tubes with 2-mm internal diameters and located at 100-mm intervals. A pressure scanner is applied for total pressure measurement, with scanning range of -17.2 kPa~17.2 kPa and accuracy rating of 0.3%.

The acoustic measurements are conducted with two B&K microphones covered by a mesh, which filters out turbulence pressure fluctuations but allows for the transmission of acoustic waves. One microphone is located at about 11 meters upstream of the rotor, and the other one is located at about 13 meters downstream of the stator. The measuring range of each microphone is 0-160 dB, with accuracy of 0.1dB. The data recording time is 10 s, and the sampling frequency is 51.2 kHz.

4 Results and Discussion

4.1 Aerodynamic Performance

The total pressure loss throughout the 5.5- by 4-m acoustic wind tunnel is larger than expected because of the roughness brought by the acoustic treatment covered on the corner vanes. Adapted to the increasing fan head rise during startup, the fan blade setting angle is adjusted at the beginning of the test, and the final rotor blade setting angle at the fan hub is 40.88 °.

To obtain the fan efficiency under typical wind tunnel operational conditions, the total pressure rise is measured at different flow velocities in each type of test section. For the solid wall test section, the fan rotational speed (N) is varied from 150 rpm to 355 rpm, and the wind speed in the test section ranges from 52.3 m/s to 130 m/s. For the open jet test section, the fan rotational speed (N) is varied from 163 rpm to 325 rpm, and the wind speed in the test section ranges from 50 m/s to 100 m/s.

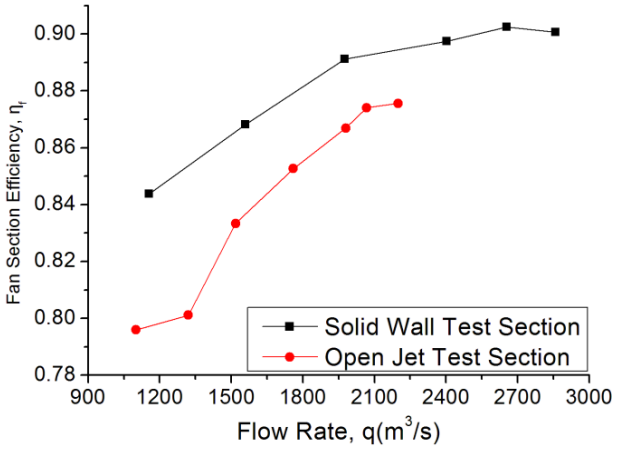

Fig.8 The fan-section efficiency as a function of flow rate

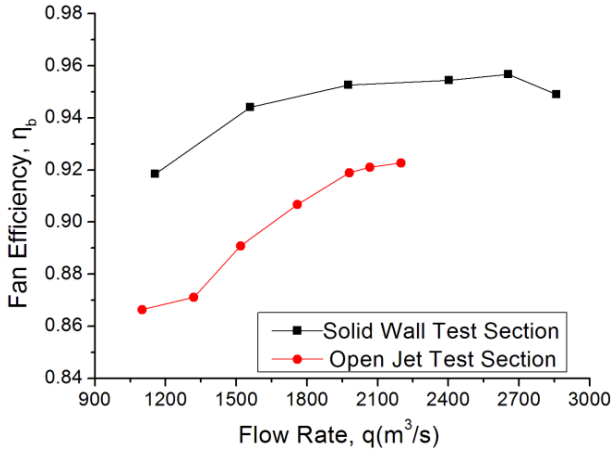

Fig.9 The fan efficiency as a function of flow rate

Figure 8 shows the fan-section efficiency at different flow rates for both solid wall and open jet test sections. As the flow rate increases, the fan-section efficiency increases in each type of test section. The peak fan-section efficiency reaches 90% at the flow rate of 2655 m^3/s in the solid wall test section, and the peak efficiency reaches 87.4% at the flow rate of 2060 m^3/s in the open jet test section.

The fan efficiencies for different types of test section are plotted in Figure 9. As expected, the fan efficiency increases with the increase of flow rate. For the solid wall test section, the fan has very high efficiency: the fan efficiency lays in the range "$91.7\% \ll \eta_b \ll 95.7\%$", and the maximum fan efficiency is reached at the flow rate of 2655 m^3/s. At the design point volume flow rate of 2860 m^3/s (corresponding to wind speed of 130 m/s in the solid wall test section), the fan efficiency is 95%, which is superior than the design requirement of 90%. For the open jet test section with wind speed 80 m/s, the fan efficiency is 90% and the flow rate is 1760 m^3/s when the rotational speed is 260 rpm.

Figure 10 presents the total pressure at the fan rotor inlet and the fan stator exit for two key wind tunnel operational points (at 130 m/s wind speed in the solid wall test section and at 80 m/s wind speed in the open jet test section). The total pressure at the stator exit is distributed more uniformly than that at the rotor inlet under both operational conditions, suggesting that the axial velocity be more uniformly distributed at the stator outlet, as predicted in the design process.

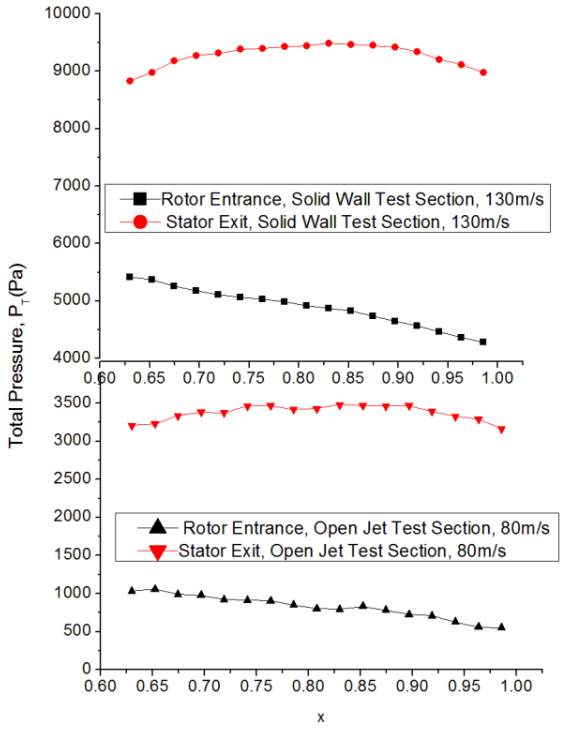

Fig.10 The total pressure distribution at different locations with different operation point

Figure 11 presents the fan total pressure rise (ΔP_T) at the two operational points mentioned above. For the solid wall test section, "ΔP_T" increases in the radial direction, and the distribution accords with the designed profile of lift coefficient (Cl, Figure 3) well. For the open jet test section, the radial distribution of "ΔP_T" shows a similar pattern of variation, except for several locations. At the location "x = 0.83", ΔP_T has a drop compared with the value of ΔP_T at the location "x = 0.81", and the value ΔP_T declines at the locations of "x = 0.92" and

" x = 0.98". The drop of ΔP_T at these locations is likely caused by the deviation of the actual velocity distribution from the designed velocity distribution at the fan inlet in the open jet test section.

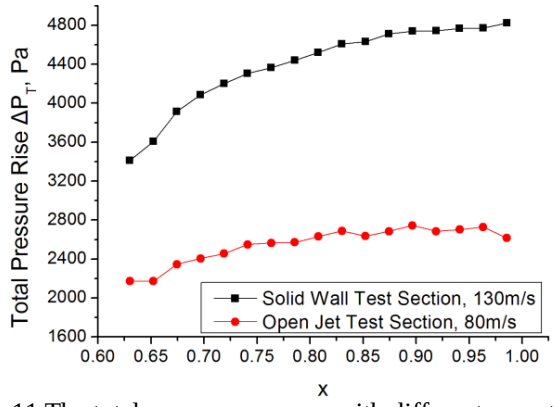

Fig.11 The total pressure versus x with different operation point

4.2 Acoustic Performance

The acoustic performance of the designed fan is tested when the wind speed is 80 m/s in the open jet test section (this wind tunnel operational point for background noise assessment follows that of the DNW-LLF wind tunnel) and the fan rotational speed is 260 rpm. The acoustic signals are analyzed after Fast-Fourier-Transform (FFT) in the range of 4 Hz to 25.6 kHz with the B & K PULSE LabShop software.

Figure 12 compares the sound pressure level in the overall frequency band at the fan inlet and fan outlet. The broadband noises at both locations have similar sound pressure levels, but the tonal noise at the fan outlet has higher sound pressure level than that at the fan inlet. At both measurement locations, the peak fan SPL is located at 144 kHz, which corresponds to the second blade passing mode. The OASPL at the fan inlet is 101 dB(A), and the OASPL at the fan outlet is 105 dB(A); both values are lower than the fan noise design target of 110 dB(A). Meanwhile, according to the results of the commissioning test of 5.5- by 4-m acoustic wind tunnel, the background noise level is 75.6 dB(A) at 80 m/s wind speed in the open jet test section, well satisfying the design requirement of 75-80 dB(A). Such low noise level also belongs to the first-class aero-acoustic wind tunnels worldwide.

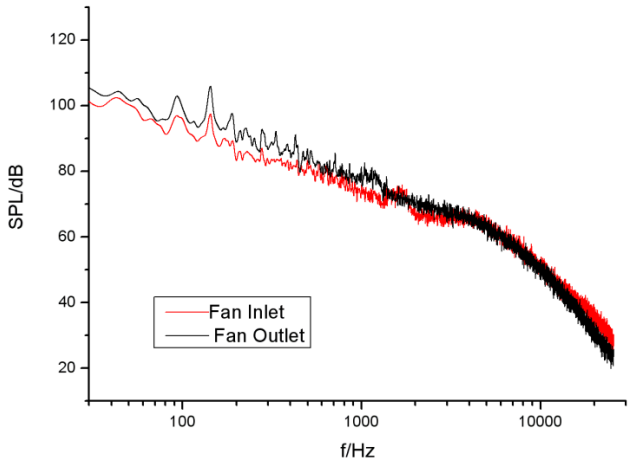

Fig12. The line octave spectra of the fan inlet and outlet for open jet test section with the wind speed 80m/s

5 Conclusions

An axial fan system is designed for the 5.5- by 4-m low speed aero-acoustic wind tunnel with closed circuit in China Aerodynamics Research and Development Center (CARDC), and the validation test results show that the designed fan has high aerodynamic performance and low noise, both successfully satisfying the design requirements.

In the design stages, the arbitrary vortex method is employed to optimize the configurations of the rotor and stator blades, and various noise reduction methods are used to reduce the fan noise. It is believed that this methodology can also be applied for the design the axial fan in other large acoustic wind tunnels.

The following lessons are learned in the design process:

(1) The arbitrary vortex method works to produce more uniform distribution of flow velocity at the outlet of fan rotor and stator, and improve the fan efficiency. The fan efficiency at the design point is 95%, which surpasses the design requirement of 90%.

(2) The methods employed for fan noise reduction effectively control the fan noise level. The first mode of blade passing frequency of the fan is successfully cut off, and the OASPL at the fan inlet and fan outlet are 9 dB(A) and 5 dB(A) lower than the design requirements, respectively.

References

[1] Edward Duell, Joel Walter, Steve Arnette, Joseph Yen. Recent Advance in Large-Scale Aeroacoustic Wind Tunnels, AIAA 2002-2503, 2002.

[2] Collar, AR. The Design of Wind Tunnel Fans. 1940.8.

[3] Pope, A. Wind-Tunnel Testing, Second Edition. John Wiley and Sons, New York.

[4] Wallis, RA. Axial flow fans and ducts. John Wiley and Sons Inc. 1983.

[5] Wallis, RA. Axial Flow Fans, Design and Practice. George Newnes Ltd, London 1961.

[6] Van Ditshuizen, JCA. Design and Calibration of the 1/10th Scale Model of the NLR Low Speed Wind Tunnel LST 8x6. AGARD CP174, Paper No. 8, 1975

[7] Tyler, JM, Sofrin, T. G. Axial Flow Compressor Noise Studies, SAE Transactions, Vol. 70, 1962, pp. 309-322.

[8] Wood Ward RP, GLASER FW. Wind tunnel measurements of blade/vane ratio and spacing effects on fan noise, Journal of Aircraft, Vol. 20, NO.1, 1983, pp. 58-65.

[9] Balombin JR, Stakolich, EG. Effect of Rotor-to-Stator Spacing on Acoustic Performance of a Full-Scale Fan (Qf-5) for Turbofan, NASA TM X-3103, E-7879, 1974.

[10] Woodward RP, Elliott DM, Hughes CE, and Berton JJ. "Benefits of Swept and Leaned Stator for Fan Noise Reduction, AIAA-99-0479, 1999.

[11] Johan BHM. Vane Sweep Effects on Rotor/Stator Interaction Noise, AIAA-96-1694, 1996.

[12] Envia E and EJ Kerchen. Influence of Vane Sweep on Rotor-Stator Interaction Noise, NASA-CR 187052, December 1990.

[13] Antoine Moreau, Sebastien Guerin, Lars Enghard. The new NWB ventilator: a practical case of design-to-noise, AIAA 2012-2178, 2012.

[14] Yu Yongsheng, Li Peng. The design specification of the 5.5m×4m Low Turbulence Aero-acoustic Wind Tunnel, CARDC Report, 2008.10

[15] Qu Xiaoli, Yu Yongsheng, Liao Daxiong, Lv jinlei. The design of the high performance low noise fan of the acoustic pilot wind tunnel, Journal of Experiments in Fluid Mechanics. Vol. 27 (3): 103-108.

[16] Wu Rongling, Wang Zhengyu. Wind Tunnel Design. 1985.3.

Copyright Statement